Large ^{14}C excursion in 5480 BC indicates an abnormal sun in the mid-Holocene

Fusa Miyake[a,1], A. J. Timothy Jull[b,c], Irina P. Panyushkina[d], Lukas Wacker[e], Matthew Salzer[d], Christopher H. Baisan[d], Todd Lange[c], Richard Cruz[c], Kimiaki Masuda[a], and Toshio Nakamura[a]

[a]Institute for Space-Earth Environmental Research, Nagoya University, Nagoya 464-8601, Japan; [b]Department of Geosciences, University of Arizona, Tucson, AZ 85721; [c]Arizona Accelerator Mass Spectrometry Laboratory, University of Arizona, Tucson, AZ 85721; [d]Laboratory of Tree Ring Research, University of Arizona, Tucson, AZ 85721; and [e]Laboratory of Ion Beam Physics, ETH Zürich, 8093 Zurich, Switzerland

Edited by Mark H. Thiemens, University of California, San Diego, La Jolla, CA, and approved December 21, 2016 (received for review August 17, 2016)

Radiocarbon content in tree rings can be an excellent proxy of the past incoming cosmic ray intensities to Earth. Although such past cosmic ray variations have been studied by measurements of ^{14}C contents in tree rings with ≥10-y time resolution for the Holocene, there are few annual ^{14}C data. There is a little understanding about annual ^{14}C variations in the past, with the exception of a few periods including the AD 774–775 ^{14}C excursion where annual measurements have been performed. Here, we report the result of ^{14}C measurements using the bristlecone pine tree rings for the period from 5490 BC to 5411 BC with 1- to 2-y resolution, and a finding of an extraordinarily large ^{14}C increase (20‰) from 5481 BC to 5471 BC (the 5480 BC event). The ^{14}C increase rate of this event is much larger than that of the normal grand solar minima. We propose the possible causes of this event are an unknown phase of grand solar minimum, or a combination of successive solar proton events and a normal grand solar minimum.

radiocarbon | cosmic ray event | solar proton event | grand solar minimum | tree rings

Cosmic rays reaching Earth are generally classified as galactic cosmic rays (GCRs) and solar cosmic rays (SCRs). GCRs including protons, heavier nuclei, electrons, gamma-ray, etc., originate from outside the heliosphere, and their intensity when they reach Earth is modulated by the interplanetary magnetic field. SCRs, which can also result from episodic solar proton events (SPEs), originate from particle acceleration in the solar corona. Incoming cosmic rays interact with Earth's atmosphere and generate an atmospheric cascade, which produces various types of particle components (1). Because cosmogenic nuclides such as ^{14}C and ^{10}Be are produced in an atmospheric cascade process, their concentrations reflect the cosmic ray intensities.

The ^{14}C contents in tree rings are normally affected by the solar magnetic activities and the geomagnetic activities, which modulate the GCR flux to Earth (2). There is an excellent tree ring record of ^{14}C data in the international radiocarbon calibration curve IntCal (3). This record has a typically 10-y resolution extending to 13,900 y B.P. We can see solar and geomagnetic variations exhibited in the radiocarbon record as decadal to millennial time scale, i.e., 50- to 100-y variation such as grand solar minima, and ∼1,000-y variations of the geomagnetic dipole moment (4).

On the other hand, there is little understanding of annual ^{14}C variations, due to the lack of annual ^{14}C data for periods before AD 1510 (5). Previously, it was considered that annual variations of ^{14}C contents do not change rapidly because the original signal is diluted and attenuated by the carbon cycle (4). Although most of annual ^{14}C data show a gradual variation, there are some periods that show significant and rapid annual changes. The AD 775 and AD 994 (or AD 993) events are two examples of large changes, which occur at annual resolution (6, 7). The ^{14}C variation of these two events have a characteristic increase over 1 y to 2 y followed by a decay that reflects a rapid input of cosmic rays to the atmosphere within 1 y and the decay by the global carbon cycle. The most likely explanation of these events is that they were the result of extreme SPEs, based on verifications of annual ^{14}C measurements using worldwide tree samples (8–11) and annual ^{10}Be measurements in ice cores from Antarctica and Greenland (12–14). It is possible that there were more annual cosmic ray events like the 775 event and even other types of annual rapid ^{14}C variation in the past.

To find more rapid changes in ^{14}C data at annual resolution, we have surveyed the periods where ^{14}C increase rates are large in the IntCal (3) record. If such annual changes occurred in the past, it is possible that such events would be manifest in the IntCal data, because a large change in 1 y to 2 y would appear in the averaged 5- to 10-y data. As a result, we have identified 15 intervals where increase rates are ≥0.3 ‰/y (using min–max values) in the IntCal13 data (3) for the Holocene (last 12,000 y) (15). The 775 event is one of these 15 intervals; the increase rate is 0.4 (‰/year). We also have the annual ^{14}C data for five other intervals, AD 1820 (6) (*SI Text*, *Annual Rapid Change in ^{14}C Records* and Fig. S1). 4680 BC, 4440 BC, 4030 BC, and 2455 BC (15), but they do not show the annual rapid changes. The 5460 BC peak from 5490 BC to 5460 BC has one of the largest increase rates (0.51‰/y) in the Holocene. We selected the period for our annual measurement for interval 5490–5411 BC to investigate the structure of the ^{14}C signal around 5460 BC.

Method and Result

We used a bristlecone pine specimen from the White Mountains (California) for annual ^{14}C measurements. Further information about the wood is provided in Fig. S2. We prepared the cellulose samples by standard chemical cleaning methods at the Accelerator Mass Spectrometry (AMS) laboratory at the University of Arizona, and measured ^{14}C contents at three different AMS

Significance

Carbon-14 contents in tree rings tell us information of the past cosmic ray intensities because cosmic rays produce ^{14}C in the atmosphere. We found a signature of a quite large increase of incoming cosmic ray intensity in the mid-Holocene (the 5480 BC event) from the measurement of ^{14}C content in North American tree rings. The cause of this event is supposed to be an extremely weak sun, or a combination of successive strong solar bursts and variation of a solar magnetic activity. In any case, ^{14}C variation of the 5480 BC event is extraordinary in the Holocene, and this event indicates the abnormal solar activity compared with other periods.

Author contributions: F.M., A.J.T.J., and I.P.P. designed research; F.M., I.P.P., L.W., M.S., C.H.B., T.L., R.C., K.M., and T.N. performed research; F.M. analyzed data; and F.M., A.J.T.J., and I.P.P. wrote the paper.

The authors declare no conflict of interest.

This article is a PNAS Direct Submission.

[1]To whom correspondence should be addressed. Email: fmiyake@isee.nagoya-u.ac.jp.

This article contains supporting information online at www.pnas.org/lookup/suppl/doi:10.1073/pnas.1613144114/-/DCSupplemental.

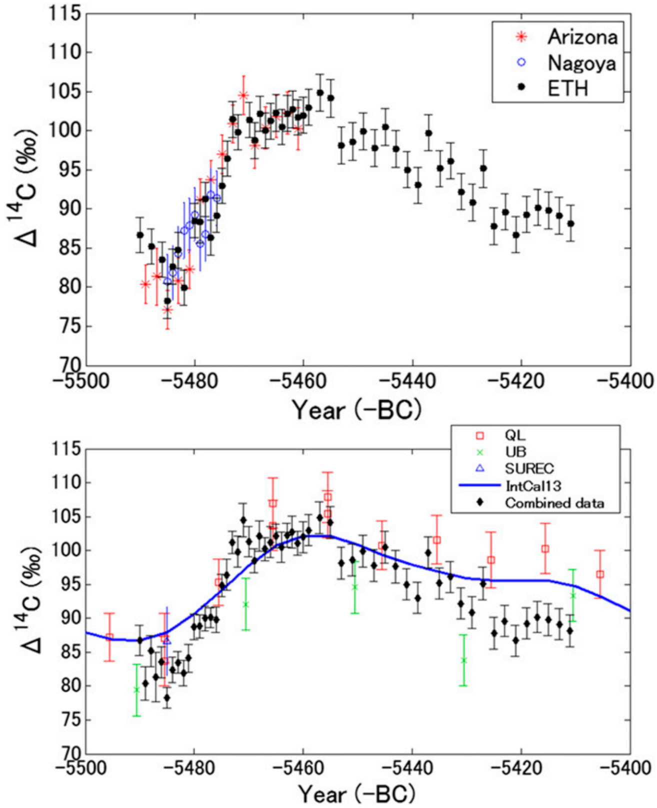

Fig. 1. (*Upper*) Measured results [$\Delta^{14}C$: defined in Stuiver and Polach (29)] of three series that were measured at different AMS laboratories (Arizona, Nagoya, and ETH). (*Lower*) Comparison of our combined data (diamonds: bristlecone pine), the original datasets of the IntCal [QL (6), UB (30), and SUREC (31)], and the IntCal13 curve (1). Although the IntCal original data are not consistent with each other, our measured results almost agree with the IntCal13.

laboratories [University of Arizona, Nagoya University, and Swiss Federal Institute of Technology (ETH)] to cross-validate our results and ascertain any laboratory offset between different AMS systems.

Fig. 1, *Upper*, shows ^{14}C results of three replicated series from our measurements. Because the three series are consistent with each other, we can immediately conclude that there are no laboratory offsets between the different AMS measurements. Because the values for the same year all agree well (Table S1), we combined the three series shown in Fig. 1, *Upper*. Fig. 1, *Lower*, shows a comparison between the combined data and the IntCal13 (3). The combined data are almost consistent with the IntCal13 and original data of the IntCal13.

From our measurements, it becomes clear that the marked increase in the IntCal13 data (5490–5460 BC) shows a very large change in annual resolution. The increase occurred from 5481 BC to 5473 BC (or 5485–5471 BC: min–max values), and the increase rates are 17.0‰/8 y (or 26.2‰/14 y), respectively. Although a variation of this event (hereafter called the 5480 BC event) is different from the previously identified events like the AD 775 event, the total increase in ^{14}C contents of the event is larger than that of the AD 775 event (~15‰). We show a comparison between the 5480 BC event and the AD 775 event in Fig. S3.

Discussion

Previous studies classified the peak around 5460 BC as a grand solar minimum, using the IntCal data (16–18). Grand solar minima are defined as the periods when the solar activity is at a very low level, i.e., it is defined as the group sunspot number becoming less than 15 during at least two consecutive decades, according to Usoskin et al. (18). In a grand solar minimum, the ^{14}C content increases largely due to a reduction of the solar modulation parameter Φ. It is estimated that Φ was ∼160 MV during the Maunder Minimum, while the present-day value varies between 400 MV and 1,000 MV (19).

We compared the annual 5480 BC event with other grand solar minima, that is the Maunder, the Spörer, the Oort, the AD seventh century, and the fourth century BC grand solar minima, where we have annual resolution ^{14}C data (5, 20–22). Fig. 2 shows a comparison between our combined datasets and other grand solar minima (more details on the grand solar minima are provided in Table S2). On average, the increase rate of the other five grand solar minima is about 0.3‰/y. Against the normal grand solar minima, the increase rate of the 5480 BC event is 2‰/y. Although the total ^{14}C increment of the 5480 BC event is almost equal to the other minima (∼20‰), the 5480 BC event increases much faster than the others. Therefore, we expect that the origin of the 5480 BC event is apparently different from the other normal grand solar minima.

To explain a rapid and large ^{14}C increase, a dramatic decrease of the solar magnetism, or extreme SPEs, is necessary. Apart from these causes, changes in the geomagnetic field can also affect the GCR flux to Earth. However, it is generally considered that the geomagnetic field does not change significantly over several centuries (4). Over ∼3,000 y from *ca.* 6000 BC to 3000 BC, the geomagnetic dipole field was ∼0.9 times smaller than today's field, and had an almost constant value (23). We do not consider the consequence of the geomagnetic effect here. Also, a change of the oceanic carbon cycle and reservoir age would affect ^{14}C; however, ocean circulation events cannot explain ^{14}C variations on a decadal scale, because these normally require up to 200 y, as shown in a study of the Younger Dryas event by Singarayer et al. (24). Whereas another galactic event, e.g., GCR flux increases for ∼10 y followed by a tail (a few decades), may explain the 5480 BC event, we do not know of any such event. Therefore, we hypothesize that plausible causes of this 5480 BC event are (*i*) special state of the grand solar minimum, (*ii*) successive extreme SPEs over ∼20 y, or (*iii*) a combination of some extreme SPEs and a normal grand solar minimum (or solar magnetic activities).

First, we consider the case of a special state of the grand solar minimum. We calculated a production rate for our measured periods using a four-box carbon cycle model (Fig. S4) with the assumption that the starting point (5484 BC) was at steady-state preindustrial value 1.8 atoms per square centimeter per second (14). Further information about the production rate is provided in *SI Text*, *Production Rate and Error Estimation*. Fig. 3 shows the

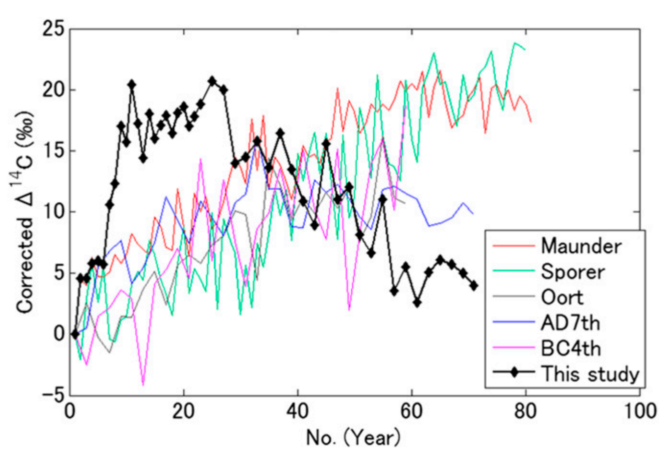

Fig. 2. Comparison of the 5480 BC event with other grand solar minima (6, 20–22). The origin of the coordinates corresponds to the shifted data point of the first year of each grand solar minima (18), and the 5481 BC data point shown in Fig. 1. Further information about the grand solar minima is provided in Table S2.

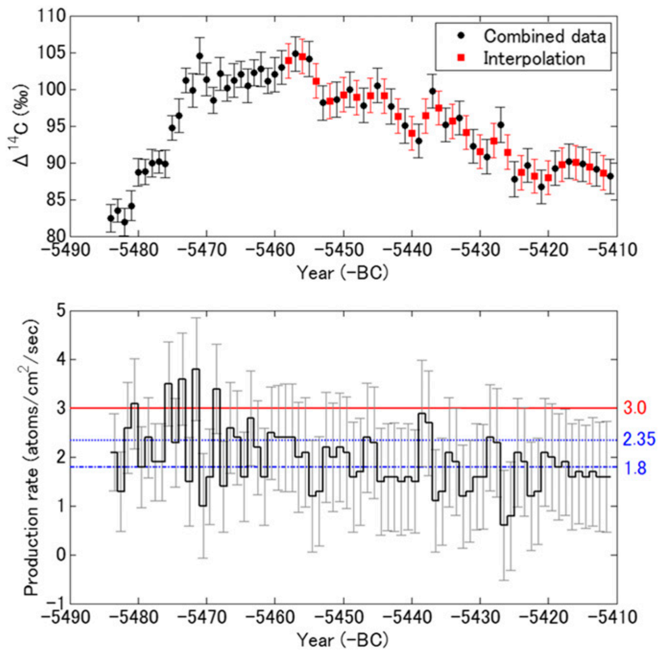

Fig. 3. The ^{14}C production rate for the period from 5484 BC to 5411 BC using a four-box model. We calculated the production rates in this graph using the steady state as 1.8 atoms per square centimeter per second. The blue dashed line (1.8 atoms per square centimeter per second) marks the production rate of normal solar magnetic activity, the blue dotted line (2.35 atoms per square centimeter per second) is average production rate for the Maunder Minimum, and the red solid line (3.0 atoms per square centimeter per second) is the production rate in the case where the solar modulation parameter becomes zero.

result of this calculated ^{14}C production rate in comparison with the $\Delta^{14}C$ data.

According to several studies, if the solar modulation parameter becomes zero, the ^{14}C production rate can increase to ∼3 atoms per square centimeter per second (19, 25, 26). Averages of the production data for the periods of 5476–5471 BC (6 y) and 5482–5471 BC (10 y) are 2.9 and 2.6 atoms per square centimeter per second, respectively. Then, the production rate during the increase period is comparable to the zero level of the solar modulation parameter. It may be difficult to explain these data only by the solar magnetic variation, because a phenomenon where the modulation parameter becomes almost zero for ∼10 y is unknown, including sun-like stars; however, we cannot fully exclude a very weak sun.

The structure of the 5480 BC event indicates a rapid increase in ^{14}C after 5470 BC followed by a gradual plateau-like increase for the next 15 y and then a gradual decay. Although the initial increase in ^{14}C for this event is different from the behavior in a normal grand solar minima, the time scale of the plateau and the following decay is consistent with the Maunder Minimum (here we have assumed the Maunder Minimum is a standard variation of a grand solar minimum; see Fig. S6). Therefore, if our event is explained only by a grand solar minimum, this means the solar activity rapidly decreased to an extremely low level, and then the solar activity became gradually higher, in a similar way to other grand solar minima.

Second, we consider the cases of successive SPEs and the combination of SPEs and solar magnetic activity. Although it is, in principle, possible that the variation is explained only by solar energetic particles over the whole period, it is less likely that the plateau and the following decay can be explained by only SPEs.

Because it is difficult to divide ^{14}C variations into the contribution by solar magnetic activities and that by SPEs, we suggest the following two scenarios: (*i*) several SPEs occurred during the early normal grand solar minimum, or (*ii*) several SPEs occurred, and then the solar magnetic activity became gradually higher. Here, we assume SPEs only occurred in the increasing period 5481–5468 BC. Knowing that a ^{14}C production rate during the Maunder Minimum varies between 2.1 atoms per square centimeter per second and 2.6 atoms per square centimeter per second (19), we can accept that a production rate for the low solar magnetic activity during the increasing ^{14}C period is an average of upper values, 2.35 atoms per square centimeter per second. In contrast, we note that the average production rate of ^{14}C during normal solar magnetic activity is 1.8 atoms per square centimeter per second. Based on these hypotheses, a total ^{14}C production by SPEs above 2.35 and 1.8 atoms per square centimeter per second during the increase can be shown to be 6.0 ± 2.4 and 10.5 ± 3.0 atoms per square centimeter per second, respectively. The total production rate of the AD 775 event has been estimated to be 3.9 atoms per square centimeter per second to 6.9 atoms per square centimeter per second (8, 10, 11, 14). Then, it is possible that the total production by SPEs of the event is comparable to or larger than the AD 775 event.

From direct measurements of the sun, we know solar flares tend to occur during a solar maximum, e.g., the number of SPEs increases in solar maximum periods (27). Also, the two annual ^{14}C events (AD 774–775 and AD 993–994) occurred in higher solar activity periods, or at least did not occur during grand solar minimum periods (7). Thus, scenario *i* (several SPEs occurred in the grand solar minimum) seems less plausible; however, the viability of one scenario over another is currently limited by our poor understanding of the mechanism for occurrence of extreme SPEs.

In the observation of solar-type stars by the Kepler telescope, stars where several superflares occurred over several years were detected (28). Such observations of solar-type stars may support an extreme SPE origin of the 5480 BC event. Further investigations of the ^{14}C record, or of other radionuclides such as annual ^{10}Be data in ice cores, may turn up similar events, which would help to further discussion of the cause of this event.

In any case, the ^{14}C variation of the 5480 BC event indicates an unprecedented anomaly in solar activity compared to other periods.

ACKNOWLEDGMENTS. We thank the staff of the Arizona Accelerator Mass Spectrometry (AMS) Laboratory and ETH AMS Laboratory for their technical assistance. We also thank Dr. H. Tajima and Dr. W. Beck for commenting on our manuscript. F.M. is supported by the Japan Society for the Promotion of Science (JSPS) Grant-in-Aid for Scientific Research (Grants 26887019 and 16H06005), JSPS Program for Advancing Strategic International Networks to Accelerate the Circulation of Talented Researchers, under Grant G2602, and Toyoaki Scholarship Foundation.

1. Burr GS (2013) Radiocarbon dating: Causes of temporal variations. *Encyclopedia of Quaternary Science*, eds Elias S, Mock CJ (Elsevier, Amsterdam), pp 336–344.
2. van der Plicht (2013) J. Radiocarbon Dating: Variations in atmospheric ^{14}C. *Encyclopedia of Quaternary Science*, eds Elias S, Mock CJ (Elsevier, Amsterdam), pp 329–335.
3. Reimer PJ, et al. (2013) IntCal13 and Marine13 radiocarbon age calibration curves, 0–50,000 years cal BP. *Radiocarbon* 55(4):1869–1887.
4. Beer J, McCracken K, Steiger R (2012) *Cosmogenic Radionuclide Theory in the Terrestrial and Space Environments* (Springer, Berlin).
5. Stuiver M, Reimer PJ, Braziunas TF (1998) High-precision radiocarbon age calibration for terrestrial and marine samples. *Radiocarbon* 40(3):1127–1151.
6. Miyake F, Nagaya K, Masuda K, Nakamura T (2012) A signature of cosmic-ray increase in AD 774-775 from tree rings in Japan. *Nature* 486(7402):240–242.
7. Miyake F, Masuda K, Nakamura T (2013) Another rapid event in the carbon-14 content of tree rings. *Nat Commun* 4:1748.
8. Usoskin IG, et al. (2013) The AD775 cosmic event revisited: The Sun is to blame. *Astron Astrophys* 552:L3.
9. Jull AJT, et al. (2014) Excursions in the ^{14}C record at A.D. 774–775 in tree rings from Russia and America. *Geophys Res Lett* 41(8):3004–3010.
10. Güttler D, et al. (2015) Rapid increase in cosmogenic ^{14}C in AD 775 measured in New Zealand kauri trees indicates short-lived increase in ^{14}C production spanning both hemispheres. *Earth Planet Sci Lett* 411:290–297.

11. Miyake F, et al. (2014) Verification of the cosmic-ray event in AD 993-994 by using a Japanese Hinoki tree. *Radiocarbon* 56(4):1–6.
12. Miyake F, et al. (2015) Cosmic ray event of A.D. 774–775 shown in quasi-annual ^{10}Be data from the Antarctic Dome Fuji ice core. *Geophys Res Lett* 42(1):84–89.
13. Sigl M, et al. (2015) Timing and climate forcing of volcanic eruptions for the past 2,500 years. *Nature* 523(7562):543–549.
14. Mekhaldi F, et al. (2015) Multiradionuclide evidence for the solar origin of the cosmic-ray events of AD 774/5 and 993/4. *Nat Commun* 6:8611.
15. Miyake F, et al. (2016) Search for annual carbon-14 excursions in the past. *Radiocarbon*, https://doi.org/10.1017/RDC.2016.54. Accessed January 9, 2017.
16. Voss H, Kurths J, Schwarz U (1996) Reconstruction of grand minima of solar activity from Δ^{14}C data: Linear and nonlinear signal analysis. *J Geophys Res* 101(A7):15,637–15,643.
17. Goslar T (2003) 14C as an indicator of solar variability. *PAGES News* 11(2-3):12–14.
18. Usoskin IG, Solanki SK, Kovaltsov GA (2007) Grand minima and maxima of solar activity: New observational constraints. *Astron Astrophys* 471(1):301–309.
19. Poluianov SV, Usoskin IG, Kovaltsov GA (2014) Cosmogenic isotope variability during the Maunder Minimum: Normal 11-year cycles are expected. *Sol Phys* 289(12): 4701–4709.
20. Miyahara H, Masuda K, Muraki Y, Kitagawa H, Nakamura T (2006) Variation of solar cyclicity during the Spoerer Minimum. *J Geophys Res* 111(A3):A03103.
21. Miyake F (2013) Reconstruction of cosmic-ray intensity in the past from measurements of radiocarbon in tree rings. Doctoral thesis (Nagoya Univ, Nagoya, Japan).
22. Nagaya K, et al. (2012) Variation of the Schwabe cycle length during the grand solar minimum in the 4th century BC deduced from radiocarbon content in tree rings. *Sol Phys* 280(1):223–236.
23. Steinhilber F, et al. (2012) 9,400 years of cosmic radiation and solar activity from ice cores and tree rings. *Proc Natl Acad Sci USA* 109(16):5967–5971.
24. Singarayer JS, et al. (2008) An oceanic origin for the increase of atmospheric radiocarbon during the Younger Dryas. *Geophys Res Lett* 35(14):L14707.
25. Castagnoli G, Lal D (1980) Solar modulation effects in terrestrial production of carbon-14. *Radiocarbon* 22(2):133–158.
26. Kovaltsov GA, Mishev A, Usoskin IG (2012) A new model of cosmogenic production of radiocarbon ^{14}C in the atmosphere. *Earth Planet Sci Lett* 337:114–120.
27. Shea MA, Smart DF (1992) Recent and historical solar proton events. *Radiocarbon* 34(2):255–262.
28. Shibayama T, et al. (2013) Superflares on solar-type stars observed with KEPLER. I. Statistical properties of superflares. *Astrophys J Suppl S* 209(1):5.
29. Stuiver M, Polach HA (1977) Discussion: Reporting of ^{14}C data. *Radiocarbon* 19(3): 355–363.
30. Pearson GW, Becker B, Qua F (1993) High-precision ^{14}C measurement of German and Irish oaks to show the natural ^{14}C variations from 7890 to 5000 BC. *Radiocarbon* 35(1): 93–104.
31. Bronk Ramsey C, et al. (2012) A complete terrestrial radiocarbon record for 11.2 to 52.8 kyr B.P. *Science* 338(6105):370–374.
32. Ferguson CW, Graybill DA (1983) Dendrochronology of bristlecone pine: A progress report. *Radiocarbon* 25(2):287–288.
33. McCormac FG, et al. (2002) Calibration of the radiocarbon time scale for the southern hemisphere: AD 1850-950. *Radiocarbon* 44(3):641–651.
34. LaMarche Jr. VC, Harlan TP (1973) Accuracy of tree ring dating of bristlecone pine for calibration of the radiocarbon time scale. *J Geophys Res* 78(36):8849–8858.
35. Miyake F, Masuda K, Nakamura T (2013) Lengths of Schwabe cycles in the seventh and eighth centuries indicated by precise measurement of carbon-14 content in tree rings. *J Geophys Res* 118(8):7483–7487.